


Accelerating discovery, enabling scientists
Discover the benefits of using spectral flow cytometry for high-parameter, high-throughput cell analysis



SONY
Download Tech Note



ZBP1/DAI Drives RIPK3-Mediated Cell Death Induced by IFNs in the Absence of RIPK1

This information is current as of August 9, 2022.

Justin P. Ingram, Roshan J. Thapa, Amanda Fisher, Bart Tummers, Ting Zhang, Chaoran Yin, Diego A. Rodriguez, Hongyan Guo, Rebecca Lane, Riley Williams, Michael J. Slifker, Suresh H. Basagoudanavar, Glenn F. Rall, Christopher P. Dillon, Douglas R. Green, William J. Kaiser and Siddharth Balachandran

J Immunol 2019; 203:1348-1355; Prepublished online 29 July 2019;
doi: 10.4049/jimmunol.1900216
<http://www.jimmunol.org/content/203/5/1348>

Supplementary Material <http://www.jimmunol.org/content/suppl/2019/07/27/jimmunol.1900216.DCSupplemental>

References This article **cites 37 articles**, 14 of which you can access for free at: <http://www.jimmunol.org/content/203/5/1348.full#ref-list-1>

Why *The JI*? Submit online.

- **Rapid Reviews! 30 days*** from submission to initial decision
- **No Triage!** Every submission reviewed by practicing scientists
- **Fast Publication!** 4 weeks from acceptance to publication

**average*

Subscription Information about subscribing to *The Journal of Immunology* is online at: <http://jimmunol.org/subscription>

Permissions Submit copyright permission requests at: <http://www.aai.org/About/Publications/JI/copyright.html>

Email Alerts Receive free email-alerts when new articles cite this article. Sign up at: <http://jimmunol.org/alerts>

The Journal of Immunology is published twice each month by
The American Association of Immunologists, Inc.,
1451 Rockville Pike, Suite 650, Rockville, MD 20852
Copyright © 2019 by The American Association of
Immunologists, Inc. All rights reserved.
Print ISSN: 0022-1767 Online ISSN: 1550-6606.



ZBP1/DAI Drives RIPK3-Mediated Cell Death Induced by IFNs in the Absence of RIPK1

Justin P. Ingram,^{*,1} Roshan J. Thapa,^{*,1} Amanda Fisher,[†] Bart Tummers,[‡] Ting Zhang,^{*} Chaoran Yin,^{*} Diego A. Rodriguez,[‡] Hongyan Guo,[†] Rebecca Lane,[†] Riley Williams,^{*} Michael J. Slifker,^{*} Suresh H. Basagoudanavar,^{*} Glenn F. Rall,^{*} Christopher P. Dillon,[‡] Douglas R. Green,[‡] William J. Kaiser,[†] and Siddharth Balachandran^{*}

Receptor-interacting protein kinase 1 (RIPK1) regulates cell fate and proinflammatory signaling downstream of multiple innate immune pathways, including those initiated by TNF- α , TLR ligands, and IFNs. Genetic ablation of *Ripk1* results in perinatal lethality arising from both RIPK3-mediated necroptosis and FADD/caspase-8–driven apoptosis. IFNs are thought to contribute to the lethality of *Ripk1*-deficient mice by activating inopportune cell death during parturition, but how IFNs activate cell death in the absence of RIPK1 is not understood. In this study, we show that Z-form nucleic acid binding protein 1 (ZBP1; also known as DAI) drives IFN-stimulated cell death in settings of RIPK1 deficiency. IFN-activated Jak/STAT signaling induces robust expression of ZBP1, which complexes with RIPK3 in the absence of RIPK1 to trigger RIPK3-driven pathways of caspase-8–mediated apoptosis and MLKL-driven necroptosis. In vivo, deletion of either *Zbp1* or core IFN signaling components prolong viability of *Ripk1*^{-/-} mice for up to 3 mo beyond parturition. Together, these studies implicate ZBP1 as the dominant activator of IFN-driven RIPK3 activation and perinatal lethality in the absence of RIPK1. *The Journal of Immunology*, 2019, 203: 1348–1355.

Receptor-interacting protein kinase 1 (RIPK1) was discovered as a serine/threonine kinase that interacted with the cytoplasmic tails of death receptors Fas/CD95 and TNFR1 (1). Subsequently, RIPK1 was also found to regulate NF- κ B and mediate cell-survival responses downstream of TNFR1 (2). In support of a survival function for RIPK1 in vivo, germline ablation of the *Ripk1* gene resulted in abrupt perinatal lethality; mice homozygously null for *Ripk1* were born at expected Mendelian frequencies but died within 48 h of birth (3).

The perinatal lethality of *Ripk1*-deficient mice remained largely unexplained for 15 y, until three studies demonstrated that this lethal phenotype could be rescued by the concurrent ablation

of both FADD/caspase-8–mediated apoptosis and RIPK3-driven necroptosis pathways (4–6). Mice triply deficient in *Ripk1*, *Ripk3*, and either *Fadd* or *Caspase-8* exhibit no overt developmental defects, matured into adulthood, are fertile, and mount robust immune responses to virus challenge (4–6). Of note, whereas activation of necroptosis in *Ripk1*^{-/-} mice is solely reliant on RIPK3, activation of FADD/caspase-8–mediated apoptosis in these mice can be either RIPK3 dependent or independent (4). The RIPK3-independent apoptotic signal is predominantly mediated by TNF- α (4, 6). However, the signal(s) responsible for activating RIPK3-mediated cell death (both necroptosis and apoptosis) in these mice are unclear. In cells, multiple innate immune signaling pathways, including those initiated by TLR3/TRIF⁻ and type I/II IFN signaling, have been shown to activate RIPK3 in settings of *Ripk1* deficiency (4, 5). As these pathways are stimulated during innate immune responses to viruses and microbes, a current model explaining the postnatal lethality of *Ripk1*-deficient mice suggests that RIPK1 restrains RIPK3-independent apoptotic death signaling by TNF- α as well as RIPK3-dependent death signaling by numerous stimuli, including type I/II IFNs, upon exposure to viruses and microbes during and after the process of mammalian parturition. It is, however, currently unclear how IFNs activate RIPK3 to drive apoptosis and necroptosis in *Ripk1*^{-/-} cells and the contribution of IFN-mediated cell death to the perinatal lethality of *Ripk1*^{-/-} mice.

In this study, we show that the ISG product ZBP1 is responsible for IFN-induced activation of RIPK3 and consequent apoptotic and necroptotic cell death in *Ripk1*^{-/-} cells. In wild-type cells, a basal RIPK1/RIPK3 complex prevents ZBP1 from associating with RIPK3, restrains RIPK3 activity, and protects cells from IFN-induced death. However, when RIPK1 expression is compromised, exposure to IFNs results in the formation of a ZBP1/RIPK3 complex that activates parallel pathways of apoptosis and necroptosis. Apoptosis is mediated by caspase-8 and proceeds independently of the kinase activity of RIPK3, whereas necroptosis is

^{*}Blood Cell Development and Function Program, Fox Chase Cancer Center, Philadelphia, PA 19111; [†]Department of Microbiology, Immunology & Molecular Genetics, UT Health Science Center at San Antonio, San Antonio, TX 78229; and [‡]Department of Immunology, St. Jude Children's Research Hospital, Memphis, TN 38105

¹Contributed equally.

ORCIDs: 0000-0002-1852-0616 (R.J.T.); 0000-0002-2634-144X (A.F.); 0000-0003-4771-0221 (D.A.R.); 0000-0002-9718-5966 (M.J.S.); 0000-0001-7714-3120 (S.H.B.).

Received for publication February 21, 2019. Accepted for publication June 27, 2019.

This work was supported by National Institutes of Health (NIH) Grants CA168621, CA190542, and AI135025 (to S.B.), Public Health Service Grant DP5OD012198 (to W.J.K.), and NIH Grants AI44828 and CA231620 (to D.R.G.). Additional funds were provided by NIH Cancer Center Support Grant P30CA006927 to the Fox Chase Cancer Center.

Address correspondence and reprint requests to: Dr. William J. Kaiser or Dr. Siddharth Balachandran, Department of Microbiology, Immunology and Molecular Genetics, UT Health Science Center at San Antonio, 7703 Floyd Curl Drive, San Antonio, TX 78229 (W.J.K.) or Blood Cell Development and Function Program, Fox Chase Cancer Center, Room 224, Reimann Building, 333 Cottman Avenue, Philadelphia, PA 19111 (S.B.). E-mail addresses: kaiserw@uthscsa.edu (W.J.K.) or Siddharth.balachandran@fccc.edu (S.B.)

The online version of this article contains supplemental material.

Abbreviations used in this article: IF, immunofluorescence; MEF, murine embryo fibroblast; RNAi, RNA interference; shRNA, short hairpin RNA; siRNA, small interfering RNA; TNFSF, TNF superfamily.

Copyright © 2019 by The American Association of Immunologists, Inc. 0022-1767/19/\$37.50

reliant on MLKL and RIPK3 activity. In vivo, the combined elimination of ZBP1 and caspase-8 extended the lifespan of *Ripk1*^{-/-} mice by over 1 mo. Furthermore, we show that elimination of components required for IFN signaling (e.g., STAT1, IFNGR1, IFNAR1, and IFNGR1+IFNAR1) phenocopy to various degrees the rescue conferred by ablation of ZBP1. Together, these results implicate ZBP1 as the dominant instigator of IFN-driven cell death during RIPK1 deficiency and identify the IFN/ZBP1 axis as an essential contributor to RIPK3 activation and perinatal lethality in *Ripk1*^{-/-} mice.

Materials and Methods

Cells and reagents

Early-passage *Ripk1*^{-/-} (3), *Ripk1*^{-/-}*Ripk3*^{-/-} (4, 5), *Zbp1*^{-/-} (7), and *Ripk1*^{-/-}*Zbp1*^{-/-} murine embryo fibroblasts (MEFs) were generated in-house from E14.5 embryos and used within five passages in all experiments. Cell viability was determined by trypan blue exclusion or on an InCuCyte Kinetic Live Cell Imaging System. Cytokines and chemicals were from the following sources: mIFN- β (PBL), mIFN- γ (R&D Systems), mTNF- α (R&D Systems), mTRAIL (R&D Systems), mGITRL (Sigma-Aldrich), z-VAD-fmk (Calbiochem), z-IETD-fmk (R&D Systems), cycloheximide (Sigma-Aldrich), actinomycin D (Maryland Biochemical), RIPK3 inhibitor GSK'843 (GlaxoSmithKline) (8), and JAK inhibitor I (Calbiochem). Abs for immunoblot analyses were obtained from MilliporeSigma (anti-MLKL and anti-JAK1), BD Biosciences (anti-STAT1 and anti-RIPK1), ProSci (anti-RIPK3 and anti-c-FLIP), Genentech (anti-p-RIPK3), Santa Cruz Biotechnology (anti-MnSOD and anti-PKR), Cell Signaling Technology (anti-caspase-8, anti-cleaved caspase-8, anti-TRAF2, and anti-p-STAT1), Abcam (anti-p-MLKL), AdipoGen Life Sciences (anti-ZBP1), and Sigma-Aldrich (anti- β -actin). The anti-p-MLKL used for immunofluorescence (IF) studies has been described before (9). The anti-cleaved caspase-8 for IF was obtained from Cell Signaling Technology. HRP-conjugated secondary Abs were obtained from Jackson ImmunoResearch Laboratories. Secondary Abs for IF were procured from Thermo Fisher Scientific. All other reagents were from Sigma-Aldrich, unless otherwise noted. All cells were cultured in high-glucose DMEM containing 10–15% FBS and antibiotics.

Mice

Zbp1^{-/-} (7), *Ripk1*^{-/-} (3), *Ripk3*^{-/-} (10), *Casp8*^{-/-} (11), *Tnfr1*^{-/-} (12), *Ifnar1*^{-/-} (13), *Ifngr1*^{-/-} (14), *Stat1*^{-/-} (15), *Sting*^{-/-} (16), and *Mavs*^{-/-} (17) mice have been previously described. Crosses were produced and genotyped by tail clip PCR, as described earlier (5). Wild-type (C57BL/6J) mice were obtained from The Jackson Laboratory. Mice were bred and maintained at the Fox Chase Cancer Center, UT Health Science Center at San Antonio, and St. Jude Children's Research Hospital in accordance with protocols approved by the respective institutional animal care and use committees of these institutions.

RNA interference

For acute RNA interference (RNAi), wild-type MEFs (5×10^5 per condition) were seeded into six-well plates and transfected with pools of four proprietary small interfering RNAs (siRNAs) (SMARTpool; Dharmacon) to the specific target mRNA at 25 nM using Oligofectamine (Invitrogen) as a transfection reagent. Nontargeting (scrambled) siRNAs (Dharmacon) were used as controls. Cells were used 72 h postinfection for experiments. For stable RNAi, prepackaged short hairpin RNA (shRNA)-expressing lentiviral particles (Sigma-Aldrich) were used. At least four distinct shRNAs per target were tested for knockdown efficiency by immunoblot analysis. The most efficient shRNAs were used to generate at least two individual stable populations of MEFs for experimental use.

Coimmunoprecipitation

MEFs (5×10^5 per condition) were harvested in lysis buffer [1% (v/v) Triton X-100, 150 mM NaCl, 20 mM HEPES (pH 7.3), 5 mM EDTA, 5 mM NaF, 0.2 mM NaVO₃ (ortho), and complete protease inhibitor mixture (Roche)]. After clarification of lysates by centrifugation, 2 μ g of Ab was added to each sample, followed by rotating incubation at 4°C overnight. Samples were then supplemented with protein A/G agarose slurry (40 μ L), incubated for 2 h, and washed four times in ice-cold lysis buffer, and bound proteins were eluted by boiling in SDS sample buffer. Eluted proteins were resolved by SDS-PAGE and analyzed by immunoblotting, as described previously (18).

IF microscopy

MEFs were plated on eight-well glass slides (MilliporeSigma) and allowed to adhere for at least 24 h before use in experiments. Following IFN treatment, cells were fixed with freshly prepared 4% (w/v) paraformaldehyde, permeabilized in 0.2% (v/v) Triton X-100, blocked with MAXblock Blocking Medium (Active Motif), and incubated overnight with primary Abs at 4°C. After three washes in PBS, slides were incubated with fluorophore-conjugated secondary Abs for 1 h at room temperature. Following an additional three washes in PBS, slides were mounted in ProLong Gold Antifade Reagent (Invitrogen) and imaged by confocal microscopy on a Leica SP8 instrument. Primary Abs were used at the following dilutions: anti-p-mMLKL (1:7000) and anti-cleaved caspase-8 (1:500).

Statistics

Statistical significance was determined by use of Student *t* test. Any *p* values ≤ 0.05 were considered significant. Graphs were generated using GraphPad Prism 6.0 software.

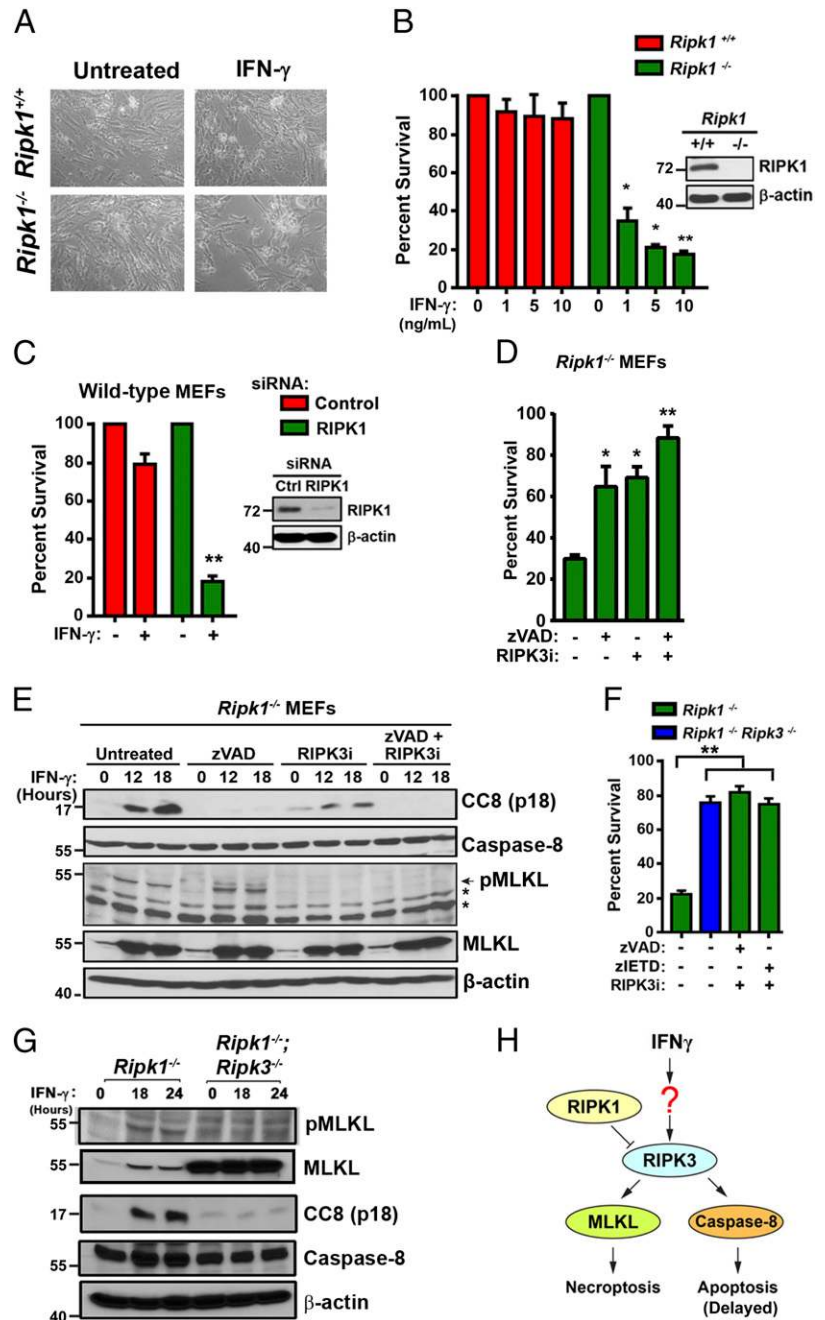
Results

IFN- γ activates RIPK3-driven parallel pathways of necroptosis and apoptosis in *Ripk1*^{-/-} MEFs

We and others have previously demonstrated that IFN- γ is toxic to primary MEFs lacking RIPK1, but the mechanism by which IFN- γ activated cell death was unclear (4, 5, 19). To examine this phenomenon further, early-passage *Ripk1*^{-/-} MEFs and wild-type littermate control MEFs were treated with IFN- γ (10 ng/ml). Cell death was monitored over a time course of 48 h, by which time *Ripk1*^{-/-} MEFs were mostly dead, whereas wild-type MEFs were largely unaffected (Fig. 1A). IFN- γ triggered cell death at dosages as low as 1 ng/ml (Fig. 1B). Similar results were observed with type I IFNs (IFN- α/β ; Supplemental Fig. 1A). Acute siRNA-mediated knockdown of RIPK1 expression in wild-type MEFs sensitized these cells to IFN- γ -induced cell death at levels comparable to those seen in *Ripk1*^{-/-} MEFs (Fig. 1C). Combined inhibition of caspase activity and RIPK3 kinase function protected *Ripk1*^{-/-} MEFs from IFN- γ (Fig. 1D), as well as from type I IFNs (Supplemental Fig. 1B), whereas neither caspase inhibition nor RIPK3 kinase blockade were singly capable of fully rescuing *Ripk1*^{-/-} MEFs from IFN- γ -induced cell death. In agreement with these observations, IFN- γ was found to activate both caspase-8 and MLKL in *Ripk1*^{-/-} MEFs (Fig. 1E). Interestingly, a kinetic analysis of caspase-8 and MLKL activation in IFN-exposed *Ripk1*^{-/-} MEFs showed that MLKL was activated more rapidly, and to a greater extent, than caspase-8 (Supplemental Fig. 1C, 1D). The pan-caspase inhibitor zVAD on its own efficiently prevented caspase-8 activation, and a RIPK3 kinase inhibitor blocked MLKL phosphorylation; expectedly, the combination of these agents prevented activation of both caspase-8 and MLKL (Fig. 1E). Notably, *Fadd*^{-/-} MEFs are also very susceptible to IFN-induced cell death, but in these cells, zVAD had no protective effect, whereas RIPK3 kinase blockade was singly capable of fully protecting against IFN- γ (Supplemental Fig. 2A). In agreement, IFN- γ treatment of *Fadd*^{-/-} MEFs induced phosphorylation of MLKL but did not detectably activate caspase-8 (Supplemental Fig. 2B). Thus, IFNs activate both necroptosis and apoptosis in *Ripk1*^{-/-} MEFs, but only necroptosis in *Fadd*^{-/-} MEFs. It is noteworthy that *Fadd*^{-/-} MEFs were also protected from IFN-induced cell death by the RIPK1 inhibitor necrostatin-1 (Supplemental Fig. 2A), suggesting that IFNs activate necroptosis by different mechanisms depending on the presence or absence of RIPK1 (see *Discussion*).

Although it is known that IFN-induced necroptosis requires RIPK3 and MLKL (4, 5, 19), it remains unclear whether apoptosis induction also relies on RIPK3. In other scenarios, for example, upon IAV infection, RIPK3 can simultaneously activate both apoptosis and necroptosis (20). To test if RIPK3 was upstream of

FIGURE 1. IFNs activate RIPK3-dependent apoptosis and necroptosis in the absence of RIPK1. **(A)** Photomicrographs of *Ripk1*^{+/+} and *Ripk1*^{-/-} MEFs treated with murine rIFN- γ (10 ng/ml) for 36 h. **(B)** *Ripk1*^{+/+} and *Ripk1*^{-/-} MEFs were treated with the indicated doses of mIFN- γ , and cell viability was determined at 36 h. RIPK1 protein expression was confirmed by immunoblotting (inset). **(C)** *Ripk1*^{+/+} MEFs were transfected with nonspecific or RIPK1-specific siRNAs. After 48 h of transfection, cells were treated with IFN- γ (10 ng/ml), and cell viability was determined 36 h posttreatment. Knockdown of RIPK1 expression was confirmed by immunoblotting (inset). **(D)** *Ripk1*^{-/-} MEFs were treated with IFN- γ (10 ng/ml) in the presence or absence of pan-caspase inhibitor z-VAD (25 μ M) and/or 5 μ M RIPK3 kinase inhibitor (GSK'843). Cell viability was determined 36 h post-treatment. **(E)** *Ripk1*^{-/-} MEFs treated with IFN- γ (10 ng/ml) in the presence of zVAD (50 μ M), GSK'843 (5 μ M), or both inhibitors together were examined for cleaved caspase-8 p18 subunit (CC8) or p-MLKL by immunoblot analysis at the indicated times. **(F)** *Ripk1*^{-/-} and *Ripk1*^{-/-}*Ripk3*^{-/-} double-knockout MEFs were treated with IFN- γ (10 ng/ml), and cell viability was determined after 36 h. In parallel, *Ripk1*^{-/-} MEFs were treated with IFN- γ in the presence of pan-caspase inhibitor zVAD (50 μ M) or the caspase-8 inhibitor zIETD (50 μ M) and 5 μ M RIPK3 kinase inhibitor (GSK'843). **(G)** Whole-cell lysates extracted from IFN- γ -treated *Ripk1*^{-/-} and *Ripk1*^{-/-}*Ripk3*^{-/-} double-knockout MEFs were examined for p-MLKL or CC8 (p18 subunit) by immunoblot analysis at the indicated times. **(H)** Schematic of IFN-induced cell death via RIPK3-dependent activation of both caspase-8-mediated apoptosis and MLKL-driven necroptosis in cells lacking RIPK1. In panels showing quantification of cell-survival data, viability of cells in untreated cultures was arbitrarily set to 100%. Molecular masses (in kiloDaltons) are shown to the left of immunoblots. Error bars represent mean \pm SD of technical replicates from a single experiment. In (B) and (C), statistical significance was determined by comparing IFN- γ -treated groups to untreated controls. In (D) and (F), these comparisons were made between inhibitor-treated groups to their untreated (but IFN- γ -exposed) controls. Viability and immunoblot experiments shown in this figure were performed at least three times each with similar results. * p < 0.05, ** p < 0.005.



both cell death modalities in *Ripk1*^{-/-} MEFs exposed to IFN- γ , we treated primary MEFs doubly deficient in RIPK1 and RIPK3 with IFN- γ and evaluated their capacity to undergo cell death over a 36 h timeframe. *Ripk1*^{-/-}*Ripk3*^{-/-} double-knockout MEFs were almost completely (~80%) protected from IFN- γ -induced cell death; their viability was comparable to *Ripk1*^{-/-} single knockouts treated with a RIPK3 kinase inhibitor and either pan-caspase inhibitor zVAD or the caspase-8 inhibitor zIETD (Fig. 1F). Coablating RIPK3 effectively nullified both IFN- γ -induced phosphorylation of MLKL and cleavage of caspase-8 (Fig. 1G, Supplemental Fig. 1C, 1D). Of note, diminished basal levels of MLKL are detected in the *Ripk1*^{-/-} MEFs, as was previously observed in *Fadd*^{-/-} MEFs (21), and likely represent a compensatory response to unrestrained RIPK3 activity in these cells. In agreement with this possibility, codeleting RIPK3 in *Ripk1*^{-/-} MEFs restored MLKL expression (Fig. 1G, Supplemental Fig. 1E). Together, these results demonstrate that IFNs activate RIPK3 and

drive both apoptosis and necroptosis in the absence of RIPK1. Apoptosis induced by IFNs requires caspase-8 and RIPK3 scaffold function, whereas necroptosis is mediated by MLKL and relies on RIPK3 kinase activity (Fig. 1H).

Induction of cell death by IFN- γ in *Ripk1*^{-/-} MEFs requires active Jak/STAT-mediated transcription and translation

IFN- γ typically mediates its cellular effects by activating a Jak/STAT-driven transcriptional program that induces the expression of hundreds of genes, called ISGs. After verifying that activation of Jak/STAT signaling, as measured by immunoblotting for p-STAT1, was unaltered in *Ripk1*^{-/-} MEFs (Fig. 2A), we tested if this signaling axis was necessary for IFN- γ -driven cell death responses in these cells. Pharmacological inhibition of Jak kinase activity (Fig. 2B, Supplemental Fig. 1B) or RNAi-mediated ablation of Jak1 or STAT1 expression efficiently protected *Ripk1*^{-/-} cells from IFN-triggered death (Fig. 2C). In agreement with a role

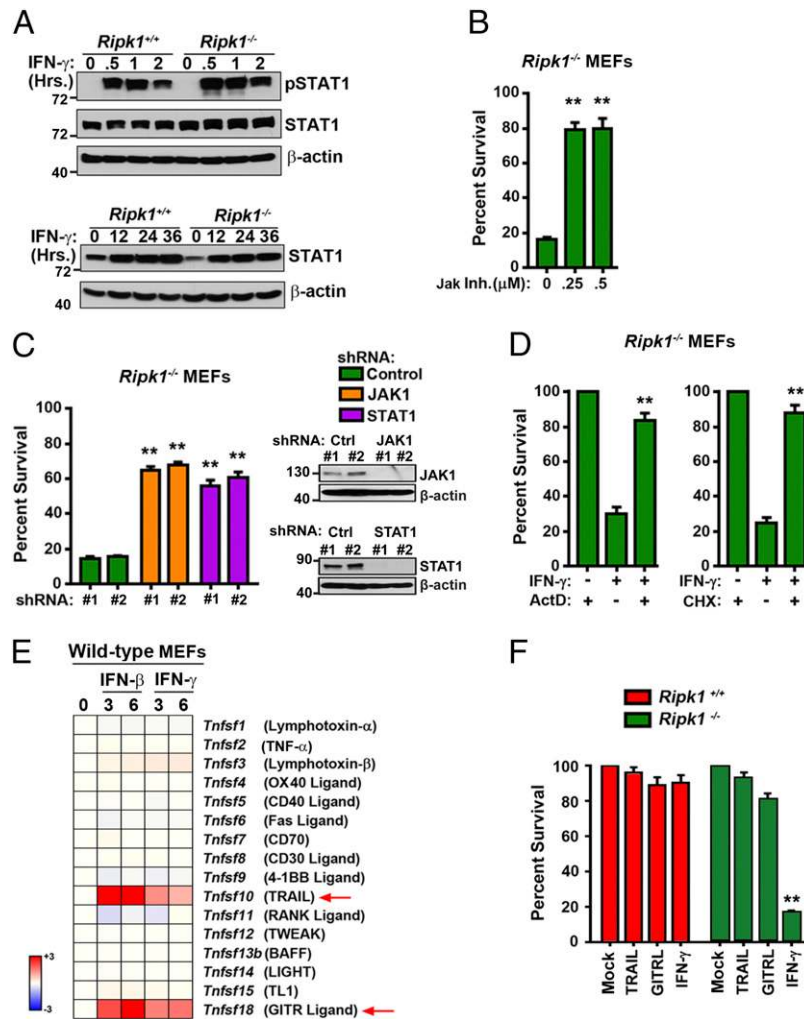


FIGURE 2. IFN-induced cell death requires Jak/STAT-mediated transcription and translation. **(A)** *Ripk1*^{+/+} and *Ripk1*^{-/-} MEFs were treated with IFN- γ (10 ng/ml) for 0.5, 1, or 2 h and were examined for p-STAT1 and STAT1 by immunoblot analysis. β -Actin was used as a loading control. In parallel, *Ripk1*^{+/+} and *Ripk1*^{-/-} MEFs were treated with IFN- γ (10 ng/ml) for 12, 24, or 36 h and were examined for STAT1 induction by immunoblot analysis. β -Actin was used as a loading control. **(B)** *Ripk1*^{-/-} MEFs were pretreated with increasing concentrations (250 and 500 nM) of JAK inhibitor I for 1 h prior to IFN- γ treatment (10 ng/ml), and cell viability was determined at 36 h. **(C)** *Ripk1*^{-/-} MEFs were transfected with nontargeting shRNAs (control) or with JAK1 or STAT1-specific shRNAs. Two distinct shRNAs (no. 1 and no. 2) were used in each case. After 48 h of transfection, cells were treated with IFN- γ (10 ng/ml), and cell viability was determined 36 h posttreatment. Knockdown of JAK1 and STAT1 expression was confirmed by immunoblotting (inset). **(D)** *Ripk1*^{-/-} MEFs were treated with IFN- γ (10 ng/ml) in the presence of actinomycin D (ActD; 25 ng/ml) or cycloheximide (CHX; 250 ng/ml), and cell viability was determined 36 h posttreatment. **(E)** TNFSF genes induced at least 2-fold by IFN- γ or IFN- β within 6 h of treatment in *Ripk1*^{-/-} MEFs were determined by DNA microarray analysis as described earlier (37). Heat bar = log₂ scale. Signal in untreated MEFs was normalized to 1 (white). **(F)** *Ripk1*^{+/+} and *Ripk1*^{-/-} MEFs were treated with mTRAIL (1 μ g/ml), mGITRL (1 μ g/ml), or mIFN- γ (10 ng/ml), and cell viability was determined after 36 h. In panels showing quantification of cell-survival data, viability of cells in untreated cultures was arbitrarily set to 100%. Molecular masses (in kiloDaltons) are shown to the left of immunoblots. Error bars represent mean \pm SD of technical replicates from one experiment. In (B) and (D), statistical significance was determined by comparing inhibitor-treated groups to their untreated (but IFN- γ -exposed) controls. In (F), statistical significance was determined by comparing cytokine-treated groups to untreated controls. Viability and immunoblot experiments shown in this figure were performed at least three times each, with similar results. ***p* < 0.005.

for ongoing transcription and translation in IFN-induced cell death, pretreatment with the RNA polymerase II inhibitor actinomycin D or the translation elongation inhibitor cycloheximide also rescued *Ripk1*^{-/-} MEFs from IFN-induced death (Fig. 2D, Supplemental Fig. 1B). These results strongly indicate that IFNs, in contrast to TNF, do not activate RIPK3 directly, but, rather, do so by inducing the expression of gene(s) that are then capable of triggering RIPK3 in *Ripk1*^{-/-} cells. These findings are consistent with our previous observations in the setting of FADD deficiency, in which IFN-induced Jak/STAT-mediated transcription and consequent activation of PKR served to initiate RIPK1/3-dependent necroptosis (19).

As IFNs induce expression of select members of the TNF superfamily (TNFSF) of cytokines, and as some TNFSFs (including

TNF- α and TRAIL) are known activators of RIPK3 (22), we next asked if IFN-induced RIPK3 activation was mediated by specific TNFSFs. To test this possibility, we first carried out DNA microarray analyses to identify which TNFSF cytokines were inducible by IFNs in MEFs. From this analysis, we determined that only TRAIL (encoded by *Tnfsf10*) and GITR ligand (*Tnfsf18*) were induced to any significant extent by either IFN- γ or IFN- β (Fig. 2E). Exposure of *Ripk1*^{-/-} MEFs to rTRAIL or GITR ligand, however, did not induce any appreciable cell death in these cells, even at a dosage (1 μ g/ml) that was 100-fold higher than a potentially cytotoxic dosage (10 ng/ml) of IFN- γ (Fig. 2F). IFN-triggered cell death in *Ripk1*^{-/-} MEFs is thus unlikely to be mediated by an IFN-inducible member of the TNFSF.

The transcription factor NF- κ B is activated by IFNs and can protect against IFN-induced necroptosis by inducing a transcriptional cell-survival program (19). As NF- κ B activation by TNF- α requires RIPK1, we next tested if IFNs also activated NF- κ B via RIPK1, and if this requirement for RIPK1 in IFN signaling might explain the susceptibility of *Ripk1*^{-/-} MEFs to IFNs. We found that, unlike the case with TNF- α , NF- κ B activation (Supplemental Fig. 3A) and induction of the NF- κ B target gene product MnSOD (Supplemental Fig. 3B) by IFN- γ was largely intact in *Ripk1*^{-/-} MEFs. Moreover TRAF2 and c-FLIP levels, shown previously to function as determinants of susceptibility to TNF- α in *Ripk1*^{-/-} MEFs (4, 6), were also unaltered by IFN- γ treatment (Supplemental Fig. 3C). These results suggest that the sensitivity of *Ripk1*^{-/-} MEFs to IFNs does not arise from defects in NF- κ B signaling.

ZBP1 activates RIPK3 after IFN stimulation of *Ripk1*^{-/-} MEFs

Having implicated JAK/STAT-driven transcription of ISGs as necessary for death of *Ripk1*^{-/-} MEFs, and having ruled out ISG-encoded TNFSF members or diminished NF- κ B transcriptional activity as possible drivers of IFN-induced cell death in these cells, we then examined if IFN-regulated innate immune sensor pathways known to stimulate RIPK3 were responsible for activating this kinase upon exposure to IFNs. Multiple innate pathways

have been shown to trigger necroptosis, including those initiated by TLR3/4, cGAS, RLRs, ZBP1, and PKR (19, 22, 23), and signaling nodes in each of these pathways are ISGs (Fig. 3A). We therefore screened each of these pathways by CRISPR and genetic approaches to test if they accounted for RIPK3 activation in *Ripk1*^{-/-} MEFs. We found that elimination of PKR (encoded by *EIF2AK2*) was able to only modestly protect *Ripk1*^{-/-} MEFs from IFNs (Supplemental Fig. 4A), in contrast to our previous results implicating this kinase in IFN-activated necroptosis in *Fadd*^{-/-} MEFs (19) (see Discussion). However, we discovered that deletion of the gene *Zbp1* was able to almost completely prevent IFN-induced cell death *Ripk1*^{-/-} MEFs (Fig. 3B, 3D). *Ripk1*^{-/-}*Zbp1*^{-/-} double-knockout MEFs from two separate crosses remained ~80% viable 48 h after exposure to IFN- γ or IFN- β , whereas <40% *Ripk1*^{-/-} MEFs were alive at this time (Fig. 3B, 3D). *Ripk1*^{-/-}*Zbp1*^{-/-} double-knockout MEFs remained as susceptible to TNF- α -mediated apoptotic death as *Ripk1*^{-/-} MEFs, demonstrating that, in the absence of RIPK1, ZBP1 is uniquely required to activate cell death upon stimulation by IFNs, but not TNF- α (Fig. 3B). RIPK1 and protein levels in each of the MEF populations used in this study are shown in Fig. 3C. Although IFN- γ induced MLKL phosphorylation in *Ripk1*^{-/-} cells, *Ripk1*^{-/-}*Zbp1*^{-/-} double-knockout MEFs had almost-undetectable levels of p-MLKL following IFN

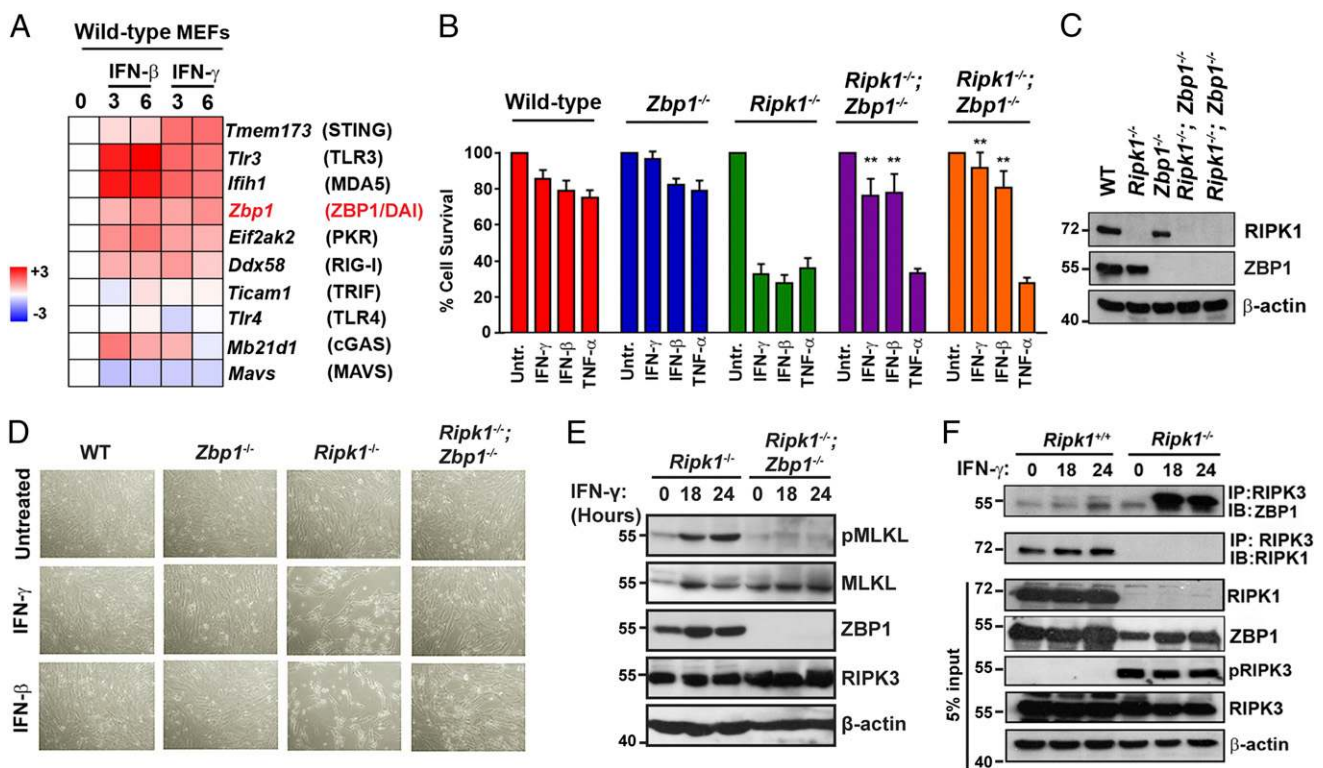


FIGURE 3. ZBP1 mediates IFN-induced RIPK3 activation and cell death in *Ripk1*^{-/-} MEFs. (A) Heatmap showing IFN inducibility of necroptosis-activating innate pathway genes. MEFs were treated with IFN- β or IFN- γ for 3 or 6 h, and the indicated genes ranked by fold induction following treatment in *Ripk1*^{+/+} MEFs. Heat bar = log₂ scale. Signal in untreated MEFs was normalized to 1 (white). (B) Wild-type, *Ripk1*^{-/-}, *Zbp1*^{-/-}, and two different *Ripk1*^{-/-}*Zbp1*^{-/-} MEFs were treated with IFN- γ (10 ng/ml), IFN- β (10 ng/ml), or TNF- α (10 ng/ml), and cell viability was determined 36 h posttreatment. (C) Wild-type, *Ripk1*^{-/-}, *Zbp1*^{-/-}, and *Ripk1*^{-/-}*Zbp1*^{-/-} MEFs from two different embryos were examined for ZBP1 and RIPK1 by immunoblotting. (D) Photomicrographs of wild-type, *Ripk1*^{-/-}, *Zbp1*^{-/-}, and *Ripk1*^{-/-}*Zbp1*^{-/-} MEFs treated with IFN- γ (10 ng/ml) or IFN- β (10 ng/ml) for 36 h. Original magnification $\times 100$. (E) *Ripk1*^{-/-} and *Ripk1*^{-/-}*Zbp1*^{-/-} MEFs were treated with IFN- γ (10 ng/ml) for 18 or 24 h and were examined for p-MLKL by immunoblot analysis. (F) Anti-RIPK3 immunoprecipitates from IFN- γ (10 ng/ml) treated *Ripk1*^{+/+} and *Ripk1*^{-/-} MEFs were examined for the presence of ZBP1. Whole-cell extract (5% input) was examined in parallel for RIPK1 and RIPK3 proteins. Immunoblotting for β -actin was used as a loading control (C, E, and F). In panels showing quantification of cell-survival data, viability of cells in untreated cultures was arbitrarily set to 100%. Molecular masses (in kilodaltons) are shown to the left of immunoblots. Error bars represent mean \pm SD of technical replicates from one experiment. In (B), statistical significance was determined by comparing cytokine-treated *Ripk1*^{-/-}*Zbp1*^{-/-} groups to cytokine-treated *Ripk1*^{-/-} controls. Viability and immunoblot experiments shown in this figure were performed at least three times each, with similar results. ***p* < 0.005.

treatment (Fig. 3E). The deletion of *Zbp1* did not significantly impact levels of either MLKL or RIPK3 (Fig. 3E). In *Ripk1*^{-/-} cells, IFN- γ robustly promoted association of ZBP1 with RIPK3, whereas an association was not seen in *Ripk1*^{+/+} cells (Fig. 3F), although *Zbp1* was induced by IFN to the same extent in both *Ripk1*^{+/+} and *Ripk1*^{-/-} cells (Supplemental Fig. 4B). Instead, in cells containing RIPK1, a basal RIPK1/RIPK3 complex was observed that did not alter in abundance with IFN treatment (Fig. 3F). p-RIPK3 was only seen in *Ripk1*^{-/-} cells, but not in cells containing RIPK1 (Fig. 3F). As the p-RIPK3 signal in *Ripk1*^{-/-} MEFs was basally present and unaltered by exposure to IFN, it likely represents a form of autophosphorylated RIPK3 that is normally restrained by constitutive association with RIPK1 (24). Together, these results demonstrate that ZBP1 mediates cell death in IFN-exposed cells lacking RIPK1 and that RIPK1 normally functions to inhibit such death by complexing with RIPK3, preventing its autophosphorylation, and blocking its association with ZBP1.

Zbp1 deletion partially rescues RIPK3-dependent perinatal lethality of *Ripk1*^{-/-} mice

Ripk1^{-/-} mice fail to survive beyond birth because of the aberrant activation of both caspase-8-mediated apoptosis and RIPK3-mediated necroptosis (4–6). *Ripk1*^{-/-} *Casp8*^{-/-} *Ripk3*^{-/-} mice are weaned at the expected frequencies and develop normally but eventually manifest an acute lymphoproliferative syndrome because of defects in Fas-induced apoptosis of T cells (4–6). TNF- α mediates aberrant RIPK3-independent caspase-8 activation in *Ripk1*^{-/-} mice, as evidenced by the ability of *Ripk1*^{-/-} *Tnfr1*^{-/-} *Ripk3*^{-/-} triple-knockout mice, but neither *Ripk1*^{-/-} *Tnfr1*^{-/-} nor *Ripk1*^{-/-} *Ripk3*^{-/-} double-knockout mice, to survive to adulthood (4, 6). However, the signals that drive RIPK3-dependent necroptosis (and apoptosis) in settings of RIPK1 deficiency are currently unclear. Given that IFNs activate RIPK3-driven cell death in *Ripk1*^{-/-} cells (Fig. 1) and that ZBP1 mediates this cell death (Fig. 3), we next determined the contribution of ZBP1 to the RIPK3-dependent lethality of *Ripk1*^{-/-} mice. To this end, we examined the effect of *Zbp1* loss on the survival of *Ripk1*^{-/-} mice, in which the TNF- α -mediated RIPK3-independent apoptosis signal was neutralized (via codeletion of *Caspase-8*). We found that *Ripk1*^{-/-} *Casp8*^{-/-} *Zbp1*^{-/-} mice were born at the expected Mendelian frequency and survived for up to 5 wk (Fig. 4A). Thus, similar to RIPK3 deficiency, the absence of *Zbp1* suppresses the lethality of *Ripk1*^{-/-} *Casp8*^{-/-} mice at parturition; however, in contrast to *Ripk1*^{-/-} *Casp8*^{-/-} *Ripk3*^{-/-} mice, which develop into fertile adults, *Ripk1*^{-/-} *Casp8*^{-/-} *Zbp1*^{-/-} mice become severely runted within the first 3 wk and ultimately fail to thrive. Notably, a single allele of *Zbp1* is tolerated in *Ripk1*^{-/-} *Casp8*^{-/-} mice and extends the lifespan by up to 2 wk (Fig. 4B), highlighting the survival benefit of reducing ZBP1 levels below a lethal threshold. Together, these data demonstrate that ZBP1 is a dominant, but not sole, instigator of inopportune RIPK3 activity in *Ripk1*^{-/-} mice.

Eliminating IFN signaling delays RIPK3-dependent lethality of *Ripk1*^{-/-} mice

As ZBP1 is an ISG, and as both type I and type II IFNs drive RIPK3 activation via ZBP1 in *Ripk1*^{-/-} cells, we next evaluated the contribution of IFNs to aberrant RIPK3 activation in, and consequent perinatal lethality of, *Ripk1*^{-/-} mice. In these studies, aberrant TNF-induced RIPK3-independent caspase-8 activity was nullified by deletion of *Tnfr1*, which, in this context, is functionally equivalent to deleting caspase-8 (4, 6). Elimination of type I IFN signaling (*Ripk1*^{-/-} *Tnfr1*^{-/-} *Ifnar1*^{-/-}) prolonged lifespan or *Ripk1*^{-/-} mice by up to a month, and abolishing both type

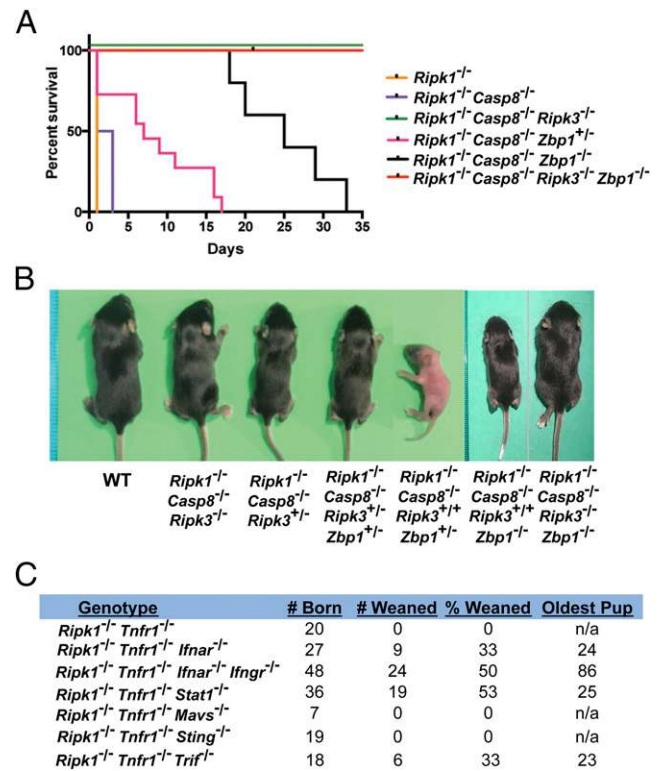


FIGURE 4. ZBP1 and IFN signaling contribute to perinatal lethality of RIPK1-deficient mice. (A) Kaplan-Meier survival plots of comparing the survival of the indicated *Ripk1*^{-/-} *Casp8*^{-/-} mice lacking one or both alleles of *Zbp1*. (B) Representative images of the indicated mice at 13 d postparturition. (C) Survival table for the indicated compound mutant mice showing number of pups weaned and age (in days) of oldest mouse at death.

I and type II IFN signaling (*Ripk1*^{-/-} *Tnfr1*^{-/-} *Ifnar1*^{-/-} *Ifngr1*^{-/-}) extended the viability of *Ripk1*^{-/-} mice for up to almost 3 mo (Fig. 4C). Interestingly, eliminating the key downstream IFN signal transducer STAT1 in this setting did not extend viability beyond 1 mo, indicating that alternate STAT1-independent IFN signals may operate to drive RIPK3 activation in *Ripk1*^{-/-} *Tnfr1*^{-/-} *Stat1*^{-/-} animals during adolescence (Fig. 4C).

Three pathogen-sensing pathways, those initiated by TLR3/4, RLRs, and cGAS, are considered the primary triggers of type I IFN production in response to viral and microbial infections, as well as to endogenous ligands during sterile inflammation, in most cell types (25). To examine if any of these pathways were responsible for lethal IFN production during parturition of *Ripk1*^{-/-} mice, we eliminated genes encoding key nodes in each of these pathways (*Trif* for TLR3/4 signaling, *Mavs* for RLRs, and *Sting* for cGAS) in *Ripk1*^{-/-} *Tnfr1*^{-/-} mice and monitored progeny for viability. Singly eliminating either *Mavs* or *Sting* did not provide any survival benefit to *Ripk1*^{-/-} *Tnfr1*^{-/-} mice, indicating that RLRs and cGAS are each redundant for RIPK3 activation and consequent lethality in *Ripk1*^{-/-} *Tnfr1*^{-/-} mice. Interestingly, deleting *Trif* extended the lifespan of *Ripk1*^{-/-} *Tnfr1*^{-/-} mice by about 1 mo, phenocopying deletion of *Ifnar1* in these animals (Fig. 4C). Although these results are suggestive of an important role for TLR3/4 signaling in production of lethal IFN in *Ripk1*^{-/-} *Tnfr1*^{-/-} mice, an alternative, and indeed more likely, explanation for the protective effects conferred by deleting *Trif* is that TRIF can directly activate RIPK3 independently of its role in IFN production (26, 27). Altogether, these data implicate IFNs as key instigators of lethal RIPK3 activation in *Ripk1*^{-/-} mice.

Discussion

We have previously shown that IFNs can activate RIPK3-dependent cell death in the absence of RIPK1 (4, 5), but the molecular mechanisms by which IFN signaling stimulates RIPK3 activity have remained unclear. In this study, we identify ZBP1 as the dominant upstream activator of IFN-induced RIPK3-dependent cell death in settings of RIPK1 deficiency. IFNs, via canonical Jak/STAT signaling, induce the expression of ZBP1, which, if RIPK1 is absent, associates with RIPK3 and triggers cell death signaling. Under steady-state conditions in wild-type MEFs, a basal association between RIPK1 and RIPK3 restrains RIPK3 to prevent association with ZBP1. Even when ZBP1 levels are boosted by IFN stimulation, RIPK1 can prevent formation of the ZBP1/RIPK3 complex and wild-type MEFs survive IFN exposure. When RIPK1 is absent, or when its RHIM is deleted (24, 28), RIPK3 is no longer restricted and is licensed to associate with ZBP1 (this study). Under these conditions, elevation of ZBP1 mRNA and protein levels following exposure to IFNs results in formation of a ZBP1/RIPK3 complex that induces both necroptosis, mediated by MLKL, and delayed apoptosis via caspase-8. It will be interesting to test if IRF-1, shown previously to mediate *Zbp1* induction during virus infections (29), and to synergize with STAT1 in the induction of a subset of ISGs (30), is required for IFN-induced *Zbp1* expression.

How does ZBP1 activate RIPK3 in the absence of RIPK1? The simplest explanation is that merely elevating ZBP1 levels in *Ripk1*^{-/-} MEFs is sufficient to promote association with free RIPK3 (i.e., RIPK3 no longer held in check by RIPK1), and this association now clusters sufficient amounts of RIPK3 to trigger kinase activation, phosphorylation of MLKL, and, ultimately, cell death. In this regard, it is noteworthy that *Ripk1*^{-/-} MEFs display constitutively autophosphorylated RIPK3, as do MEFs expressing a RHIM-mutant version of RIPK1 (24). These observations indicate that RIPK1, via a RHIM/RHIM interaction with RIPK3, suppresses RIPK3 activity. In the absence of RIPK1, RIPK3 autophosphorylates and becomes available for interaction with other RHIM-containing proteins, including ZBP1. Under these circumstances, stimuli (such as IFNs) that boost levels of ZBP1 promote RHIM-dependent oligomerization between ZBP1 and RIPK3 to trigger death signaling.

ZBP1 also has direct nucleic acid sensing capacity (20, 31–34), so an alternate, albeit more complex, explanation is that IFN induction of *Zbp1* expression alone is insufficient to trigger necroptosis, and that ZBP1 is instead (or additionally) activated by endogenous or pathogen-derived nucleic acids at parturition. *Zbp1* mutant knock-in mice that cannot bind nucleic acid (e.g., by mutations in the α nucleic acid-sensing domains) but still retain the ability to associate with RIPK3 will help distinguish between these alternatives.

An unanticipated outcome from these studies was the finding that, in primary MEFs, IFNs activated necroptosis by notably different mechanisms depending on whether RIPK1 was absent or present. In *Fadd*^{-/-} MEFs, for example, IFNs drove a pathway of necroptosis that was reliant on PKR and, in remarkable contrast to *Ripk1*^{-/-} MEFs, required the kinase activity of RIPK1. Moreover, *Fadd*^{-/-} MEFs did not display either significant basal levels of autophosphorylated RIPK3 or evidence of an IFN-stimulated RIPK3 complex (data not shown); instead, *Fadd*^{-/-} MEFs contained a preformed necrosome complex, composed of phosphorylated forms of RIPK1 and RIPK3, that drove necroptosis upon exposure to IFNs (19). Downstream of RIPK3 activation, we were surprised to observe that, in addition to necroptosis, a pathway of apoptosis reliant on caspase-8 was also induced in *Ripk1*^{-/-} MEFs. Although RIPK3 has been previously shown to activate

caspase-8, such activation was found to require RIPK1 as a bridging adaptor protein necessary for recruitment of caspase-8 to RIPK3. How RIPK3 can activate caspase-8 in the absence of RIPK1 is currently unclear, but suggests the involvement of an as-yet unidentified adaptor(s) that substitutes for RIPK1 in linking RIPK3 to caspase-8. Of interest in this study, RIPK3 was found to interact with not just caspase-8, but with several other caspases, including caspases-2, -9, and -10 (35). All these caspases have large prodomains, but some [such as caspase-9, with which RIPK3 associates robustly (35)] do not possess the death effector domains (DEDs) required for association with FADD and RIPK1. Thus, RIPK3 can associate with caspases by DED-independent (and, therefore, likely FADD/RIPK1-independent) mechanisms. In this regard, we observed that RIPK3 activated caspase-8 with notably slower kinetics than it did MLKL (Supplemental Fig. 1D), indicating that a secondary transcriptional event may be required for caspase-8 activation by RIPK3.

It is noteworthy that, although ablating ZBP1 expression extended the life of *Ripk1*^{-/-} *Caspase-8*^{-/-} mice for up to 5 wk, eliminating RIPK3 in these mice can protect against lethality for more than a year (4–6). These observations indicate that ZBP1-independent signals later in life trigger RIPK3 when RIPK1 is absent. Activation of the TLR3/4 pathway might represent one such signal, as the TLR3/4 adaptor protein TRIF can directly engage RIPK3 via a RHIM/RHIM association, independent of its capacity to stimulate IFN production (26, 27). It is also likely that other as-yet undescribed mechanisms of RIPK3 activation likely exist; in this regard, Silverman and colleagues (36) have shown the existence of RHIM-like sequences in the *Drosophila* proteins PGRP-LC, PGRP-LE, and IMD that can functionally reconstitute RHIM-based signaling in mammalian cells. Whether mammalian proteins with similar cryptic RHIMs function to trigger RIPK3 in adulthood awaits discovery.

In aggregate, our results implicate IFNs as dominant triggers of RIPK3 activation when RIPK1 is absent, and demonstrate that IFNs activate RIPK3 by inducing expression of ZBP1. RIPK1 protects cells from IFN-mediated toxicity by restraining RIPK3 activity and preventing RIPK3 from associating with ZBP1. Thus, RIPK1 functions in development as a homeostatic harbor by protecting against lethal IFN-mediated cell death signaling without impeding beneficial host defense responses induced by these cytokines upon exposure to viruses and microbes during and after parturition.

Acknowledgments

We thank Anthony Lerro, Lauren Heisey, and Simon Tarpanian for animal husbandry and Maria Shubina for help preparing figures.

Disclosures

The authors have no financial conflicts of interest.

References

1. Stanger, B. Z., P. Leder, T. H. Lee, E. Kim, and B. Seed. 1995. RIP: a novel protein containing a death domain that interacts with Fas/APO-1 (CD95) in yeast and causes cell death. *Cell* 81: 513–523.
2. Hsu, H., J. Huang, H. B. Shu, V. Baichwal, and D. V. Goeddel. 1996. TNF-dependent recruitment of the protein kinase RIP to the TNF receptor-1 signaling complex. *Immunity* 4: 387–396.
3. Kelliher, M. A., S. Grimm, Y. Ishida, F. Kuo, B. Z. Stanger, and P. Leder. 1998. The death domain kinase RIP mediates the TNF-induced NF- κ B signal. *Immunity* 8: 297–303.
4. Dillon, C. P., R. Weinlich, D. A. Rodriguez, J. G. Cripps, G. Quarato, P. Gurung, K. C. Verbist, T. L. Brewer, F. Llambi, Y. N. Gong, et al. 2014. RIPK1 blocks early postnatal lethality mediated by caspase-8 and RIPK3. *Cell* 157: 1189–1202.
5. Kaiser, W. J., L. P. Daley-Bauer, R. J. Thapa, P. Mandal, S. B. Berger, C. Huang, A. Sundararajan, H. Guo, L. Roback, S. H. Speck, et al. 2014. RIP1 suppresses innate immune necrotic as well as apoptotic cell death during mammalian parturition. *Proc. Natl. Acad. Sci. USA* 111: 7753–7758.

6. Rickard, J. A., J. A. O'Donnell, J. M. Evans, N. Lalaoui, A. R. Poh, T. Rogers, J. E. Vince, K. E. Lawlor, R. L. Ninnis, H. Anderton, et al. 2014. RIPK1 regulates RIPK3-MLKL-driven systemic inflammation and emergency hematopoiesis. *Cell* 157: 1175–1188.
7. Ishii, K. J., T. Kawagoe, S. Koyama, K. Matsui, H. Kumar, T. Kawai, S. Uematsu, O. Takeuchi, F. Takeshita, C. Coban, and S. Akira. 2008. TANK-binding kinase-1 delineates innate and adaptive immune responses to DNA vaccines. *Nature* 451: 725–729.
8. Mandal, P. S. B. Berger, S. Pillay, K. Moriwaki, C. Huang, H. Guo, J. D. Lich, J. Finger, V. Kasparcova, B. Votta, et al. 2014. RIP3 induces apoptosis independent of proinflammatory kinase activity. *Mol. Cell* 56: 481–495.
9. Rodriguez, D. A., R. Weinlich, S. Brown, C. Guy, P. Fitzgerald, C. P. Dillon, A. Oberst, G. Quarato, J. Low, J. G. Cripps, et al. 2016. Characterization of RIPK3-mediated phosphorylation of the activation loop of MLKL during necroptosis. *Cell Death Differ.* 23: 76–88.
10. Newton, K., X. Sun, and V. M. Dixit. 2004. Kinase RIP3 is dispensable for normal NF- κ B signaling by the B-cell and T-cell receptors, tumor necrosis factor receptor 1, and Toll-like receptors 2 and 4. *Mol. Cell Biol.* 24: 1464–1469.
11. Salmena, L., B. Lemmers, A. Hakem, E. Matsiyak-Zablocki, K. Murakami, P. Y. Au, D. M. Berry, L. Tamblyn, A. Shehabeldin, E. Migon, et al. 2003. Essential role for caspase 8 in T-cell homeostasis and T-cell-mediated immunity. *Genes Dev.* 17: 883–895.
12. Pfeffer, K., T. Matsuyama, T. M. Kündig, A. Wakeham, K. Kishihara, A. Shahinian, K. Wiegmann, P. S. Ohashi, M. Krönke, and T. W. Mak. 1993. Mice deficient for the 55 kd tumor necrosis factor receptor are resistant to endotoxic shock, yet succumb to *L. monocytogenes* infection. *Cell* 73: 457–467.
13. Müller, U., U. Steinhoff, L. F. Reis, S. Hemmi, J. Pavlovic, R. M. Zinkernagel, and M. Aguet. 1994. Functional role of type I and type II interferons in antiviral defense. *Science* 264: 1918–1921.
14. Huang, S., W. Hendriks, A. Althage, S. Hemmi, H. Bluethmann, R. Kamijo, J. Vilcek, R. M. Zinkernagel, and M. Aguet. 1993. Immune response in mice that lack the interferon-gamma receptor. *Science* 259: 1742–1745.
15. Meraz, M. A., J. M. White, K. C. Sheehan, E. A. Bach, S. J. Rodig, A. S. Dighe, D. H. Kaplan, J. K. Riley, A. C. Greenlund, D. Campbell, et al. 1996. Targeted disruption of the Stat1 gene in mice reveals unexpected physiologic specificity in the JAK-STAT signaling pathway. *Cell* 84: 431–442.
16. Ishikawa, H., Z. Ma, and G. N. Barber. 2009. STING regulates intracellular DNA-mediated, type I interferon-dependent innate immunity. *Nature* 461: 788–792.
17. Sun, Q., L. Sun, H. H. Liu, X. Chen, R. B. Seth, J. Forman, and Z. J. Chen. 2006. The specific and essential role of MAVS in antiviral innate immune responses. *Immunity* 24: 633–642.
18. Chen, P., S. Nogusa, R. J. Thapa, C. Shaller, H. Simmons, S. Peri, G. P. Adams, and S. Balachandran. 2013. Anti-CD70 immunocytokines for exploitation of interferon- γ -induced RIP1-dependent necrosis in renal cell carcinoma. *PLoS One* 8: e61446.
19. Thapa, R. J., S. Nogusa, P. Chen, J. L. Maki, A. Lerro, M. Andrade, G. F. Rall, A. Degterev, and S. Balachandran. 2013. Interferon-induced RIP1/RIP3-mediated necrosis requires PKR and is licensed by FADD and caspases. *Proc. Natl. Acad. Sci. USA* 110: E3109–E3118.
20. Thapa, R. J., J. P. Ingram, K. B. Ragan, S. Nogusa, D. F. Boyd, A. A. Benitez, H. Sridharan, R. Kosoff, M. Shubina, V. J. Landsteiner, et al. 2016. DAI senses influenza A virus genomic RNA and activates RIPK3-dependent cell death. *Cell Host Microbe* 20: 674–681.
21. Nogusa, S., R. J. Thapa, C. P. Dillon, S. Liedmann, T. H. Oguin, III, J. P. Ingram, D. A. Rodriguez, R. Kosoff, S. Sharma, O. Sturm, et al. 2016. RIPK3 activates parallel pathways of MLKL-driven necroptosis and FADD-mediated apoptosis to protect against influenza A virus. *Cell Host Microbe* 20: 13–24.
22. Vanden Berghe, T., B. Hassannia, and P. Vandenabeele. 2016. An outline of necrosome triggers. *Cell. Mol. Life Sci.* 73: 2137–2152.
23. Upton, J. W., M. Shubina, and S. Balachandran. 2017. RIPK3-driven cell death during virus infections. *Immunol. Rev.* 277: 90–101.
24. Newton, K., K. E. Wickliffe, A. Maltzman, D. L. Dugger, A. Strasser, V. C. Pham, J. R. Lill, M. Roose-Girma, S. Warming, M. Solon, et al. 2016. RIPK1 inhibits ZBP1-driven necroptosis during development. *Nature* 540: 129–133.
25. Wu, J., and Z. J. Chen. 2014. Innate immune sensing and signaling of cytosolic nucleic acids. *Annu. Rev. Immunol.* 32: 461–488.
26. Kaiser, W. J., H. Sridharan, C. Huang, P. Mandal, J. W. Upton, P. J. Gough, C. A. Sehon, R. W. Marquis, J. Bertin, and E. S. Mocarski. 2013. Toll-like receptor 3-mediated necrosis via TRIF, RIP3, and MLKL. *J. Biol. Chem.* 288: 31268–31279.
27. He, S., Y. Liang, F. Shao, and X. Wang. 2011. Toll-like receptors activate programmed necrosis in macrophages through a receptor-interacting kinase-3-mediated pathway. *Proc. Natl. Acad. Sci. USA* 108: 20054–20059.
28. Lin, J., S. Kumari, C. Kim, T. M. Van, L. Wachsmuth, A. Polykratis, and M. Pasparakis. 2016. RIPK1 counteracts ZBP1-mediated necroptosis to inhibit inflammation. *Nature* 540: 124–128.
29. Kuriakose, T., M. Zheng, G. Neale, and T. D. Kanneganti. 2018. IRF1 is a transcriptional regulator of ZBP1 promoting NLRP3 inflammasome activation and cell death during influenza virus infection. *J. Immunol.* 200: 1489–1495.
30. Ramsauer, K., M. Farlik, G. Zupkovic, C. Seiser, A. Kröger, H. Hauser, and T. Decker. 2007. Distinct modes of action applied by transcription factors STAT1 and IRF1 to initiate transcription of the IFN- γ -inducible gbp2 gene. *Proc. Natl. Acad. Sci. USA* 104: 2849–2854.
31. Upton, J. W., W. J. Kaiser, and E. S. Mocarski. 2012. DAI/ZBP1/DLM-1 complexes with RIP3 to mediate virus-induced programmed necrosis that is targeted by murine cytomegalovirus vIRA. *Cell Host Microbe* 11: 290–297.
32. Kuriakose, T., S. M. Man, R. K. Malireddi, R. Karki, S. Kesavardhana, D. E. Place, G. Neale, P. Vogel, and T. D. Kanneganti. 2016. ZBP1/DAI is an innate sensor of influenza virus triggering the NLRP3 inflammasome and programmed cell death pathways. *Sci. Immunol.* 1: aag2045.
33. Koehler, H., S. Cotsmire, J. Langland, K. V. Kibler, D. Kalman, J. W. Upton, E. S. Mocarski, and B. L. Jacobs. 2017. Inhibition of DAI-dependent necroptosis by the Z-DNA binding domain of the vaccinia virus innate immune evasion protein, E3. *Proc. Natl. Acad. Sci. USA* 114: 11506–11511.
34. Guo, H., R. P. Gilley, A. Fisher, R. Lane, V. J. Landsteiner, K. B. Ragan, C. M. Dovey, J. E. Carette, J. W. Upton, E. S. Mocarski, and W. J. Kaiser. 2018. Species-independent contribution of ZBP1/DAI/DLM-1-triggered necroptosis in host defense against HSV1. *Cell Death Dis.* 9: 816.
35. Sun, X., J. Lee, T. Navas, D. T. Baldwin, T. A. Stewart, and V. M. Dixit. 1999. RIP3, a novel apoptosis-inducing kinase. *J. Biol. Chem.* 274: 16871–16875.
36. Kleino, A., N. F. Ramia, G. Bozkurt, Y. Shen, H. Nailwal, J. Huang, J. Napetschnig, M. Gangloff, F. K. Chan, H. Wu, et al. 2017. Peptidoglycan-sensing receptors trigger the formation of functional amyloids of the adaptor protein Imd to initiate Drosophila NF- κ B signaling. *Immunity* 47: 635–647.e6.
37. Basagoudanavar, S. H., R. J. Thapa, S. Nogusa, J. Wang, A. A. Beg, and S. Balachandran. 2011. Distinct roles for the NF- κ B RelA subunit during antiviral innate immune responses. *J. Virol.* 85: 2599–2610.